Electronic Supplementary Material (ESI) for Journal of Materials Chemistry A.

Supporting Information

Optimizing Na Metal/Solid Electrolyte Interface through a Grain Boundary Design

Chengzhi Wang, Chen Sun, Boyu Wang, Zheng Sun, Tinglu Song, Yongjie Zhao, Jingbo Li, Haibo Jin*

Experimental Section

Synthesis of the solid electrolyte: A liquid-phase sintering method is adopted to synthesize the grain boundary sealed $Na_3Zr_2Si_2PO_{12}$ (denote as GBS-NZSP) solid electrolyte using $(ZnO)_2$-$(B_2O_3)_3$ additive in the molar ratio range of x=0-0.3. Firstly, raw materials of anhydrous Na_2CO_3, $ZrO(NO_3)_2$, SiO_2, $NH_4H_2PO_4$, ZnO, B_2O_3 are stoichiometrically mixed with 10% sodium excess by a high-speed agitator. The raw mixture is pre-sintered at 1000 ℃ for 12 h. Then, the pre-sintered powder was pressed into pellets of 11 mm in diameter with the assistance of a polyvinyl butyral (PVB) binder, which was subsequently pyrolyzed at 650 ℃ for 3 h in air. Finally, sintering of the pellets is conducted at 1000 ℃ for 12 h with a ramp rate of 5 ℃ min^{-1}. Additionally, as comparison, normally sintered $Na_3Zr_2Si_2PO_{12}$ is also prepared by only shifting the final sintering temperature to 1250 ℃ without using any additive and the as-obtained sample is named as NZSP-1250. All the synthesized solid electrolyte pellets are gradually polished by silicon carbide abrasive papers of #600, #1000, #1500, #2000, #3000 until a smooth and clean surface appears and a thickness of around 1.0 mm is reached.

Synthesis of the cathode material: The cathode material of $Na_3V_{1.5}Cr_{0.5}(PO_4)_3$ (NVCP) is synthesized via a sol-gel method. Typically, raw chemicals of $C_6H_5Na_3O_7$, V_2O_3, $Cr(NO_3)_3$ and $NH_4H_2PO_4$ with a stoichiometric ratio are firstly dissolved in deionized water. After stirring at 80 ℃ for 12 h, a dried precursor gel forms and is subsequently calcinated at 800 ℃ for 10 h in Ar flow to obtain the NVCP cathode material.

Synthesis of the plastic-crystal electrolyte: The plastic-crystal electrolyte is prepared as an ionic conductive additive of the cathode. Typically, 0.1 mmol of $NaClO_4$ is dissolved in 2 mmol of succinonitrile at 65 °C to form a clear solution. After cooling to room temperature, a yellow and sticky plastic-crystal electrolyte is obtained.

Characterization: X-ray diffraction (XRD, Bruker D8 advance) is used to analyze the phase structure. Field emission scanning electron microscope (FESEM, Hitachi Regulus8230) equipped with an energy dispersive spectrometer (EDS) and field emission transmittance electron microscope (FETEM, FEI Tecnai F30) are adopted for microstructural and composition characterization. A TGA-DSC synchronous thermal analyzer (Mettler Toledo TGA/DSC 1) is used to obtain the thermal property under air flow. Surface chemical states are analysed by X-ray photoelectron spectroscopy (XPS, Thermo Scientific *K*-Alpha). The depth profile of surface components is measured by Time of Flight Secondary Ion Mass Spectrometry (ToF-SIMS, PHI nano TOF II). For XPS and TOF-SIMS characterization, the Ar-protected sample injection is performed using a transition chamber through an Ar-filled glove box.

Electrochemical test: All-solid-state CR2032-type symmetrical cells of Na//Na are assembled using a hydraulic coin-cell crimping machine (HF-Kejing, MSK-110, 50 MPa crimping pressure) in an Ar-filled glovebox by directly placing sodium foils on both sides of the solid electrolyte disc without any pre- or post-treatment. Galvanostatic cycling of the symmetrical cells is conducted on a multi-channel battery test system at 25 ℃ controlled by an incubator. CR2032-typed solid-state sodium metal batteries of NVCP//Na are assembled by using PCE-NVCP composite as cathode, Na foil as the anode, and GBS-NZSP (x=0.2) as the solid electrolyte. The composite cathode is fabricated by mixing NVCP, carbon black, polyvinylidene fluoride (PVDF) and the plastic-crystal electrolyte at a weight ratio of 60: 5: 10: 25 in a mortar with N-methyl-2-pyrrodione (NMP) as a solvent. The obtained slurry is casted on the current collector of aluminum foil. After drying at room temperature for 48 h under vacuum, the coated Al foil is punched into discs of 6 mm in diameter with the active mass loading of about 1.5 mg cm^{-2}. Electrochemical impedance spectroscopy (EIS) analysis was conducted in the frequency range of 0.1-1 MHz with an amplitude of 5 mV on a CHI660E electrochemical workstation to reveal the charge transfer at the interfaces. The activation energy for interfacial conductivity is verified according to *Arrhenius* equation. An eight-channel battery test system (Land CT3001A) is used to measure the galvanostatic cycling profile of the solid-state sodium batteries at room temperature.

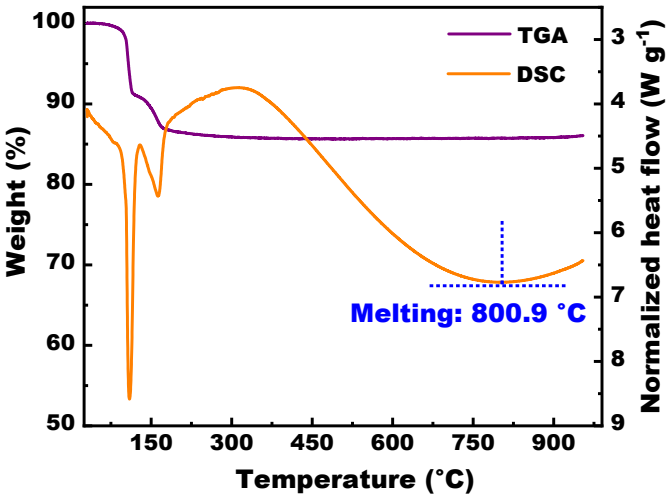

Fig. S1 TGA-DSC curves of $(ZnO)_2$-$(B_2O_3)_3$.

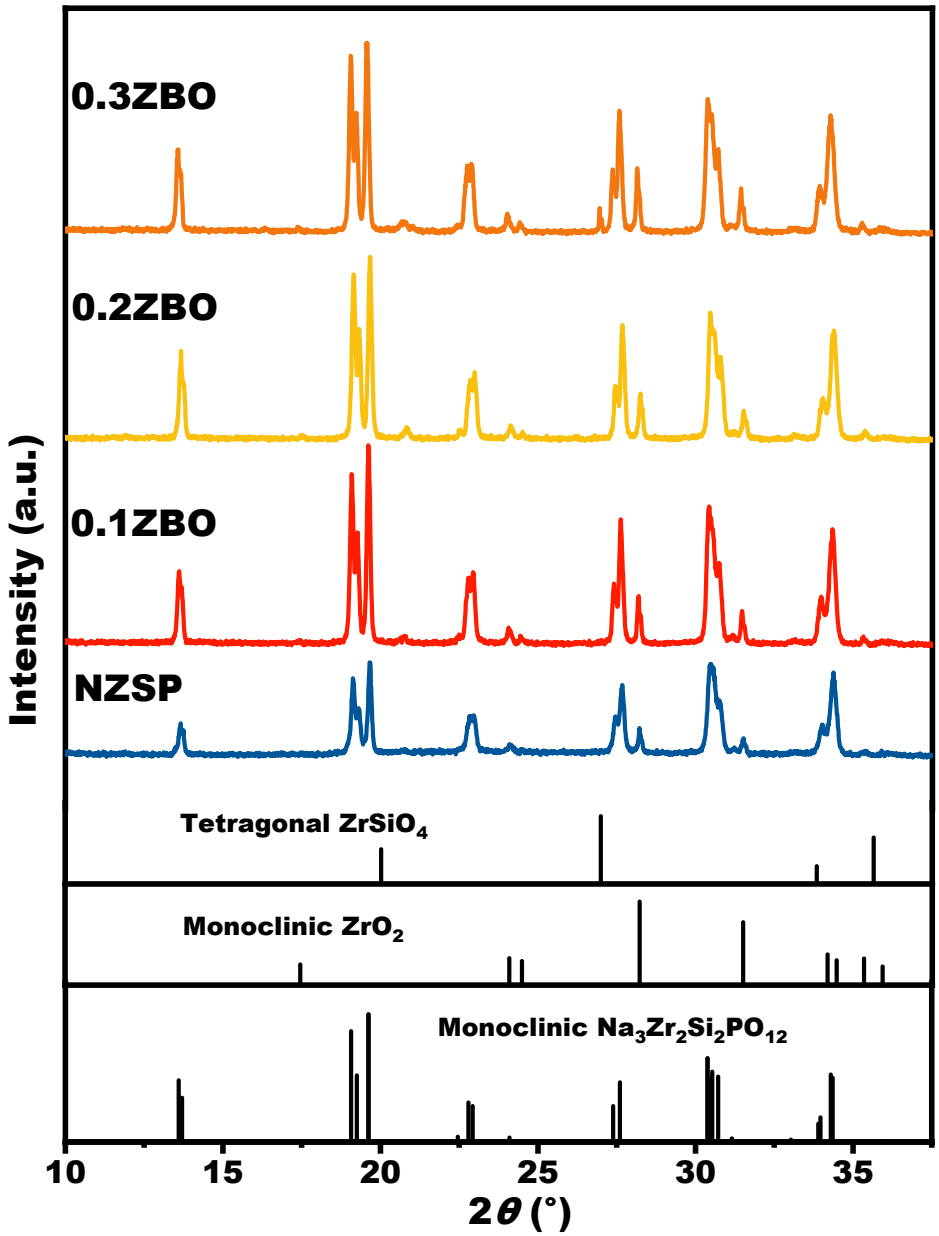

Fig. S2 XRD patterns of bare NZSP and GBS-NZSP samples with ZBO content *x* variation.

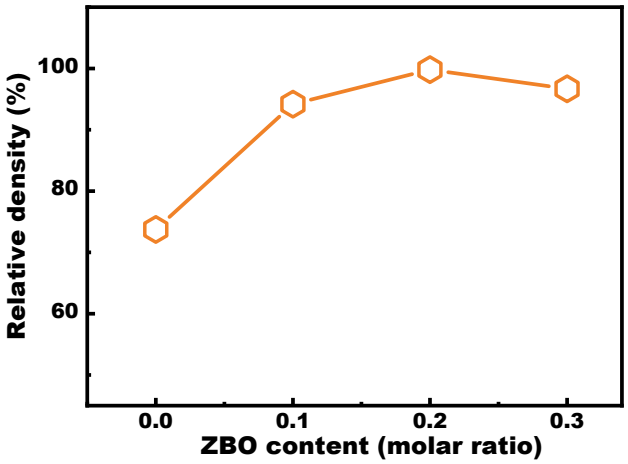

Fig. S3 Relative densities of bare NZSP and GBS-NZSP samples with ZBO content *x* variation.

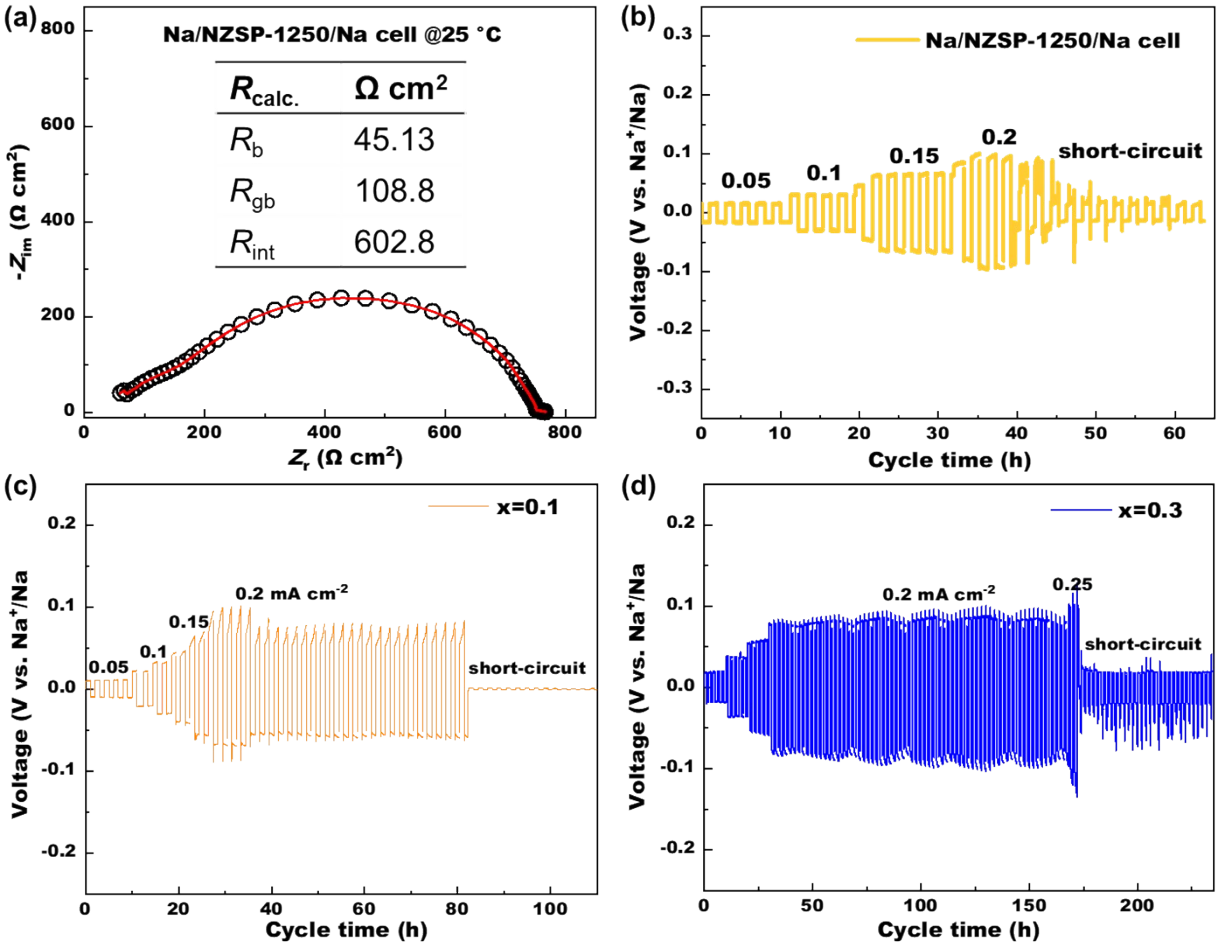

Fig. S4 (a) Nyquist plots and calculated R_b, R_{gb}, R_{int} of the Na/NZSP-1250/Na cell. Galvanostatic cycling profile of Na//Na symmetrical cells using (b) NZSP-1250, (c) GBS-NZSP (x=0.1) and (d) GBS-NZSP (x=0.3) as solid electrolytes under stepwise increased current densities at room temperature.

Table S1. Room-temperature electrochemical performance of all-solid-state symmetrical Na//Na cells using $Na_3Zr_2Si_2PO_{12}$-based solid electrolytes.

Metal/Solid electrolyte interfaces	Cell /interfacial resistance (Ω cm^2)	CCD (mA cm^{-2})	Cycling stability (mA cm^{-2}/h)	Ref.
Na/$Na_3Zr_2Si_2PO_{12}$ by solution sintering	105/64.5	0.3	0.1/800	1
Na/$Na_{3.1}Zr_{1.95}Mg_{0.05}Si_2PO_{12}$	NA	NA	0.044/50	2
Na/post-treated $Na_3Zr_2Si_2PO_{12}$ at 450 ℃	680/636	NA	0.1/1450	3
Na/TiO_2-coated $Na_3Zr_2Si_2PO_{12}$	350/101	NA	0.1/860	4
Na/SnO_2-trilayer-$Na_{3.2}Zr_{1.9}Ca_{0.1}Si_2PO_{12}$	175/NA	NA	0.3/600 h	5
Na-SiO_2/$Na_3Zr_2Si_2PO_{12}$	575/101	0.5	0.1-0.2/135	6
Na/SPAN-$Na_3Zr_2Si_2PO_{12}$	387.4/NA	1.4	0.15-0.25/500	7
Na/TS-$Na_3Zr_2Si_2PO_{12}$	350/129	0.4	0.1/2100 0.2/1000	8
Ultrasound welding Na/$Na_3Zr_2Si_2PO_{12}$	140/22.6	0.6	0.1/1300 0.2/400	9
Na/GBS-$Na_3Zr_2Si_2PO_{12}$	131/27	0.55	0.3/1400	This work

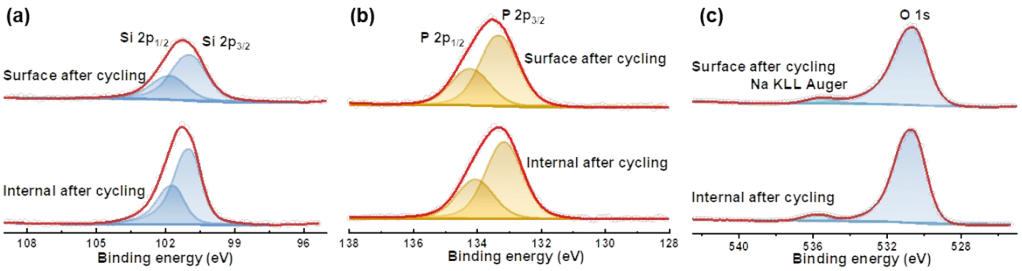

Fig. S5. XPS spectra of (a) Si 2p, (b) P 2p and (c) O 1s collected from the surface and internal section of NZSP-0.2ZBO after Na plating/stripping cycles.

Table S2. Structural parameters for $Na_3V_{1.5}Cr_{0.5}(PO_4)_3$ based on lab XRD data collected at room temperature refined in space group R-3c (No 167) using Rietveld analysis. Cell parameters a = 8.7306(7) Å, b = 8.7306(7) Å, c = 21.8216(92) Å, γ = 120.000º, volume = 1440.50(4) Å^3.

	x	*y*	*z*	Occ.	U	Site	Sym.
V1	0.33333	0.66667	0.01954	0.667	0.010	12c	3.0
Na1	0.33333	0.66667	0.16667	0.805	0.013	6b	-3.0
Na2	0.66667	0.9673	0.08333	0.731	0.022	18e	0.2
P1	-0.04196	0.33333	0.08333	1.000	0.010	18e	0.2
O1	0.14259	0.49874	0.07847	1.000	0.010	36f	1.0
O2	0.54378	0.84527	-0.02608	1.000	0.010	36f	1.0
Cr	0.33333	0.66667	0.01954	0.333	0.010	12c	3.0

Phase agreement: R_{wp}=10.5%, R_p=9.8%, χ^2=1.98.

Table S3. Room-temperature electrochemical performance of solid-state full sodium metal cells using $Na_3Zr_2Si_2PO_{12}$-based solid electrolytes.

Cell configuration	Cycling performance	Rate performance	Ref.
NVP-LE|$Na_3Zr_2Si_2PO_{12}$-TiO_2|Na	0.1 C/70.6% after 60 cycles	NA	4
NVP/SCN/PEO/$NaClO_4$)|$Na_{3.2}Zr_{1.9}Ca_{0.1}Si_2PO_{12}$ SnO_2-trilayer|Na	1 C/98.13% after 450 cycles	4 C/80.5 mA h g^{-1}	5
NVP-LE|$Na_3Zr_2Si_2PO_{12}$-SPAN|Na	0.5 C/87.5% after 200 cycles	2 C/81.1 mA h g^{-1}	7
NVCP/PCE|$Na_3Zr_2Si_2PO_{12}$-TS|Na	100 mA g^{-1}/73% after 400 cycles	100 mA g^{-1}/103 mA h g^{-1}	8
NVP-LE|$Na_3Zr_2Si_2PO_{12}$|Na-UW	0.1 mA cm^{-2}/89.81% after 900 cycles	0.5 mA cm^{-2}/93 mA h g^{-1}	9
NVCP/PCE|GBS-$Na_3Zr_2Si_2PO_{12}$|Na	10 C/81% after 560 cycles	10 C/108 mA h g^{-1}	This work

References

1 Z. Zhang, S. Wenzel, Y. Zhu, J. Sann, L. Shen, J. Yang, X. Yao, Y.-S. Hu, C. Wolverton, H. Li, L. Chen, J. Janek, *ACS Appl. Energy Mater.*, 2020, 3, 7427-7437.

2 S. Song, H.M. Duong, A.M. Korsunsky, N. Hu, L. Lu, *Sci. Rep.*, 2016, 6, 32330.

3 Z. Gao, J. Yang, H. Yuan, H. Fu, Y. Li, Y. Li, T. Ferber, C. Guhl, H. Sun, W. Jaegermann, R. Hausbrand, Y. Huang, *Chem. Mater.*, 2020, 32, 3970-3979.

4 J. Yang, Z. Gao, T. Ferber, H. Zhang, C. Guhl, L. Yang, Y. Li, Z. Deng, P. Liu, C. Cheng, R. Che, W. Jaegermann, RenéHausbrand, Y. Huang, *J. Mater. Chem. A*, 2020, 8, 7828-7835.

5 Y. Lu, J.A. Alonso, Q. Yi, L. Lu, Z.L. Wang, C.W. Sun, *Adv. Energy Mater.*, 2019, 9, 1901205.

6 H. Fu, Q. Yin, Y. Huang, H. Sun, Y. Chen, R. Zhang, Q. Yu, L. Gu, J. Duan, W. Luo, *ACS Mater. Lett.*, 2019, 2, 127-132.

7 X. Miao, H. Wang, R. Sun, X. Ge, D. Zhao, P. Wang, R. Wang, L. Yin, *Adv. Energy Mater.*, 2021, 11, 2003469.

8 C. Wang, H. Jin, Y. Zhao, *Small*, 2021, 17, 2100974.

9 X. Wang, J. Chen, D. Wang, Z. Mao, *Nat. Comm.*, 2021, 12, 7109.